

A Plane Segmentation System Based on Affine Homography and Optical Flow

Kelson Rômulo Teixeira Aires
Department of Informatics and Statistics
Federal University of Piauí, UFPI
Teresina, PI, Brazil
kelson@ufpi.edu.br

Adelardo Adelino Dantas de Medeiros
Department of Computing Engineering and Automation
Federal University of Rio Grande do Norte, UFRN
Natal, RN, Brazil
adelardo@dca.ufrn.br

Abstract—Planes are important geometric features and can be used in a wide range of vision tasks like scene reconstruction, path planning and robot navigation. This work aims to illustrate a plane segmentation system based on homography computation and optical flow estimation. Firstly, using two image frames from a monocular sequence, a set of match pairs of interest points is obtained. An algorithm was developed to cluster interest points belonging to the same plane based on the reprojection error of the affine homography. From the calculated homographies, the planar flow is computed for each image pixel. Following this, the estimated optical flow is used to expand and identify each detected plane. An optical flow estimation method based on color information is presented. Tests were performed in different sequences of indoor and outdoor images and results validate the proposed system.

Keywords-plane segmentation, optical flow, 3D reconstruction.

I. INTRODUCTION

For robot navigation, active and passive sensors are generally used. Active sensors like sonar or lasers can provide simple information about obstacle detection. The drawback is that the information is sparse. On the other hand, visual sensors provide dense information about the surrounding environment. A vision system mounted on a robot can capture an image sequence from the camera motion. This information can be used to recover the structure of the scene and to plan a free path to the robot navigation while avoiding obstacles.

Planar surfaces present within a scene can provide useful information on the environment, making the robot able of distinguishing between obstacles and ground plane. A lot of works related to plane detection are found in the literature [1], [2], [3]. In [4], the normal vector to a plane is estimated by using only three corresponding points from stereo images. A method for detecting multiple planar regions using a progressive voting procedure from the solution of a linear system exploiting the two-view geometry is presented in [5]. SIFT (Scale Invariant Feature Transform) features were used in [6] to obtain the estimates of the planar homographies which represent the motion of the major planes in the scene. They track a combined Harris and SIFT features using the prediction by these homographies.

In [7], an algorithm for the estimation of the optical flow field of the dominant plane detection from an image sequence is developed. From two successive images, correspond points on dominant plane are combined with an affine transformation. Using this, the affine coefficients are computed and the dense planar flow is obtained. Only the dominant plane is detected by matching the flow vectors. The approach presented in [2] detects three-dimensional planar surfaces using 3D Hough transformation to extract candidates to plane segment. Finally, a detailed review and performance comparisons of planar homography estimation techniques can be found in [8].

This work introduces a complete and simple system to obtain all major planes present in a scene. Using two images from a monocular image sequence, the first step is to compute a set of match pairs of points. From this set of matches a homography-based method is performed to detect planes using the affine model. Each affine homography represents a planar surface present in the scene. An algorithm was developed to cluster interest points belonging to the same plane. From the calculated homographies, the planar flow is computed for each image pixel.

Following this, the detected planes are expanded by matching the planar flow and the estimated optical flow. An optical flow estimation method based on color information is presented. A plane identification procedure is performed based on the number of pixels belonging to each plane. At the end, each segmented plane is labeled as ground plane or obstacle. Tests were performed in different sequences of indoor and outdoor images and results validate the proposed system.

The paper is organized as follows. Section 2 presents the main aspects related to the theory of two view geometry. In Section 3, an optical flow estimation method from color information is presented. In Section 4, the proposed system is formulated highlighting all crucial points. Results are shown in Section 5. Finally, Section 6 summarizes this paper and some future works are proposed.

II. TWO VIEW GEOMETRY

A. Preliminary

The pinhole model is used to describe the camera. Points are represented by homogeneous coordinates. A 3D point is represented by $\mathbf{Q} = [X \ Y \ Z \ 1]^T$ in a world coordinate system, and its retinal image coordinate is described by the 2D point $\mathbf{q} = [x \ y \ 1]^T$. The corresponding homogeneous coordinates are related by the following matricial equation

$$w\mathbf{q} = \mathbf{P}\mathbf{Q}, \quad (1)$$

where w is an unknown scale and \mathbf{P} is the perspective projection matrix.

The matrix \mathbf{P} can be decomposed as

$$\mathbf{P} = K [R \ \mathbf{t}], \quad (2)$$

where K is a 3×3 calibration matrix, mapping the normalized image coordinates to the retinal image coordinates, and (R, \mathbf{t}) describes the rotation and translation from the world frame to the camera frame.

All quantities related to the second view of the same camera are indicated by '. Thus, \mathbf{q} is a point in the first image and \mathbf{q}' is the corresponding point in the second image.

B. Planar Homography

The images of a planar object imaged from two view points are related by a homography. Consider that \mathbf{q} and \mathbf{q}' are the projections of \mathbf{Q} in the first and second view respectively. The homography \mathbf{H} is uniquely induced by the imaged plane, and describes the mapping $\mathbf{q} \leftrightarrow \mathbf{q}'$, given by

$$s\mathbf{q}' = \mathbf{H}\mathbf{q}. \quad (3)$$

where s is the scale factor.

The matrix \mathbf{H} has 9 entries, but is defined only up to scale. Each corresponding 2D point generates two constraints on \mathbf{H} by Equation 3 and hence the correspondence of four points is sufficient to compute \mathbf{H} .

1) *Affine Homography*: An affine homography \mathbf{H}_A is a special case of the planar homography. The matrix representation is formulated as

$$\mathbf{q}' = \mathbf{H}_A \mathbf{q} = \begin{bmatrix} \mathbf{A} & \mathbf{t} \\ \mathbf{0}^T & 1 \end{bmatrix} \mathbf{q}. \quad (4)$$

The affine homography \mathbf{H}_A has 6 degrees of freedom and can be computed from three point correspondences of the same plane. A modified version of *Direct Linear Transformation* method is used to estimate the homography. The Equation 3 can be formulated in terms of an inhomogeneous set of linear equations as

$$\begin{bmatrix} x_1 & y_1 & 1 & 0 & 0 & 0 \\ 0 & 0 & 0 & x_1 & y_1 & 1 \\ \vdots & & & \vdots & & \\ x_n & y_n & 1 & 0 & 0 & 0 \\ 0 & 0 & 0 & x_n & y_n & 1 \end{bmatrix} \cdot \begin{bmatrix} h_1 \\ h_2 \\ h_3 \\ h_4 \\ h_5 \\ h_6 \end{bmatrix} = \begin{bmatrix} x'_1 \\ y'_1 \\ \vdots \\ x'_n \\ y'_n \end{bmatrix}, \quad (5)$$

where $[x_i \ y_i] \leftrightarrow [x'_i \ y'_i]$, $i = 1, \dots, n$, are the matched pairs of points in inhomogeneous coordinates and \mathbf{H}_A has the form

$$\mathbf{H}_A = \begin{bmatrix} h_1 & h_2 & h_3 \\ h_4 & h_5 & h_6 \\ 0 & 0 & 1 \end{bmatrix}. \quad (6)$$

C. Reprojection error

An error measure may be considered after an affine homography \mathbf{H}_A has been computed. In order to verify whether a given matched pair of points belongs to the plane represented by \mathbf{H}_A , we use the *reprojection error*

$$e_i = |\mathbf{q}_i - \hat{\mathbf{q}}_i|^2 + |\mathbf{q}'_i - \hat{\mathbf{q}}'_i|^2, \quad (7)$$

where $\hat{\mathbf{q}}'_i = \mathbf{H}_A \mathbf{q}_i$ and $\hat{\mathbf{q}}_i = \mathbf{H}_A^{-1} \mathbf{q}'_i$.

A given matched pair $\mathbf{q}_i \leftrightarrow \mathbf{q}'_i$ belongs to the plane represented by \mathbf{H}_A when the reprojection error e_i is below a certain threshold.

III. OPTICAL FLOW FROM COLORED IMAGES

In computer vision, optical flow is a velocity field associated with image changes. This effect generally appears due to the relative movement between object and camera or by moving the light sources that illuminates the scene [9]. Most approaches to estimate optical flow are based on brightness changes between two images.

Among the existing methods for Optical Flow estimation, gradient based techniques are distinguished. Such techniques are based on image brightness changes of each pixel with (x, y) coordinates. Considering that small displacements do not modify brightness intensity of an image point, a *Constraint Optical Flow Equation* can be defined as

$$I_x u + I_y v + I_t = 0, \quad (8)$$

where u and v are the optical flow components in x and y directions for a displacement $\mathbf{d} = (dx, dy)$, I_x , I_y and I_t are the partial derivatives of the image brightness, $I(x, y)$, with regard to the horizontal (x) and vertical (y) coordinates, and time (t). Optical flow cannot be estimated only from Equation 8. Thus, some additional constraint needs to be used to find a solution for the flow components, u and v .

A. Lucas and Kanade's Method

Lucas and Kanade [10] used a local constraint to solve the aperture problem. This method considers that small regions in the image corresponds to the same object and have similar movement. The image is divided in windows of size $N \times N$, each one with $p = N^2$ pixels. A local constraint is used to form an overconstrained system with p equations and 2 variables, as in 9.

$$\begin{aligned} I_{x1}u + I_{y1}v + I_{t1} &= 0 \\ I_{x2}u + I_{y2}v + I_{t2} &= 0 \\ &\vdots \\ I_{xp}u + I_{yp}v + I_{tp} &= 0 \end{aligned} \quad (9)$$

System 9 can be solved by the Least Mean Square (LMS) method for estimating the optical flow vector. The estimated optical flow for each $N \times N$ window corresponds to the optical flow vector of all pixels in the related window.

B. Proposed Method

Color image is an additional natural resource of information that can facilitate the problem resolution. Ohta [11] was the first one to consider an optical flow estimation method that does not use additional constraints about movements in the image. His method is based on multi-channel images (as colored images) to obtain multiple constraints from a simple image pixel [12]. Barron et al [13] in their analysis showed that optical flow estimation is improved when color information is used.

The optical flow equation 8 can be applied to each image channel. A system of equations can be formulated to provide a solution to optical flow vector without additional constraints concerning image movement. For color images with three channels (RGB, HSV, HSI, YUV) the system would result in

$$\begin{aligned} I_{1x}u + I_{1y}v + I_{1t} &= 0 \\ I_{2x}u + I_{2y}v + I_{2t} &= 0 . \\ I_{3x}u + I_{3y}v + I_{3t} &= 0 \end{aligned} \quad (10)$$

In our previous work [14], we propose a method for optical flow estimation from two colored images of a sequence. This method is based on Lucas and Kanade's algorithm [10].

The image frame is divided into several observation windows of similar movement. An optical flow vector that corresponds to all pixels of the window is estimated. For optical flow estimation, only some pixels of each window are chosen equally distributed in window space.

The Equation 8 is applied to each chosen pixel of all image channels. The best results were obtained using YUV color model. A system of equations is obtained for each window, given in matricial form by

$$\mathbf{A} \cdot \mathbf{v} + \mathbf{b} = \mathbf{0}, \quad (11)$$

where $\mathbf{v} = [u \ v]^T$ is the optical flow vector, \mathbf{A} is the spacial partial derivates matrix and \mathbf{b} is the temporal derivates vector.

The System 11 can be solved by pseudo-inverse method, as

$$\mathbf{v} = (\mathbf{A}^T \mathbf{A})^{-1} \cdot (\mathbf{A}^T \mathbf{b}). \quad (12)$$

In Equation 11, the $\mathbf{A}^T \mathbf{A}$ matrix must be non-singular. The condition number n of $\mathbf{A}^T \mathbf{A}$ is used to measure the numerical stability of the System 11. If n is above a certain threshold, \mathbf{v} is not defined on that image location [13].

Finally, a filter based on the euclidian distance of optical flow vectors is used. A flow vector of a $N \times N$ window is only accepted as valid if it exists at least a neighbouring

window (neighbourhood-8), where the square of the euclidian distance between the two flow vectors does not exceed 20% of the flow vector being analysed.

IV. PLANE SEGMENTATION SYSTEM

This section presents a system for segmentation of planes based on affine homographies and optical flow estimated from two colored images of a sequence. Figure 1 illustrates the detailed block diagram of the entire system. The following sections describe each part of the proposed system.

A. 2D Plane Detection

This section describes a plane detection system as used in our previous work [15]. The first step consists of obtaining a set M of matched pairs of interest points between two consecutive images of a sequence. As suggested in [16], the combination of Harris corner detector [17] with SIFT descriptor [18] was chosen.

Given M , a Delaunay triangulation [19] is performed only on the detected corners of the first image. Since the set of triangles T has been obtained, a filtering scheme is applied to discard triangles that probably belong to virtual planes in the image. Only triangles with all sides within a certain range of lengths are considered valid. Still, triangles with valid sides can have their vertices almost collinear. Collinearity of the three points used in the computation of affine homographies must be avoided. To solve this problem, triangles with areas less than a certain value are also discarded.

The new set of triangles T obtained from the filtering scheme is used by a clustering procedure to join points that belong to the same plane in the image. Using M and T , we define H_m as the set of all m homographies existing between the two images. Each homography in H_m defines a plane present in both images.

Initially H_m is considered as empty. The first affine homography \mathbf{H}_A is computed using the three points (vertexes) of the first triangle $T(1)$ and their matched points in the set M . Homography \mathbf{H}_A thus obtained is included in H_m , and all used points are marked as *visited* and assigned to the homography $H_m(1)$, i.e., the first plane.

In the next step, the next triangle of T and their corresponding matched points in M are considered. For each homography in H_m , all points of the triangle are checked to determine whether they belong to any of the existing planes in H_m . For this, if the point had been marked as *not-visited* and the reprojection error for H_i is below a certain threshold, the point is marked as *visited* and assigned to homography $H_m(i)$. If the point had been marked as *visited* and if the new reprojection error for H_i is smaller than the previous one, the point is assigned to the plane H_i . In the case where all points of the triangle do not belong to any existing plane, a new affine homography \mathbf{H}_A is computed with those points. The new homography represents a new plane and is included in H_m . This loop is performed until there are no unvisited

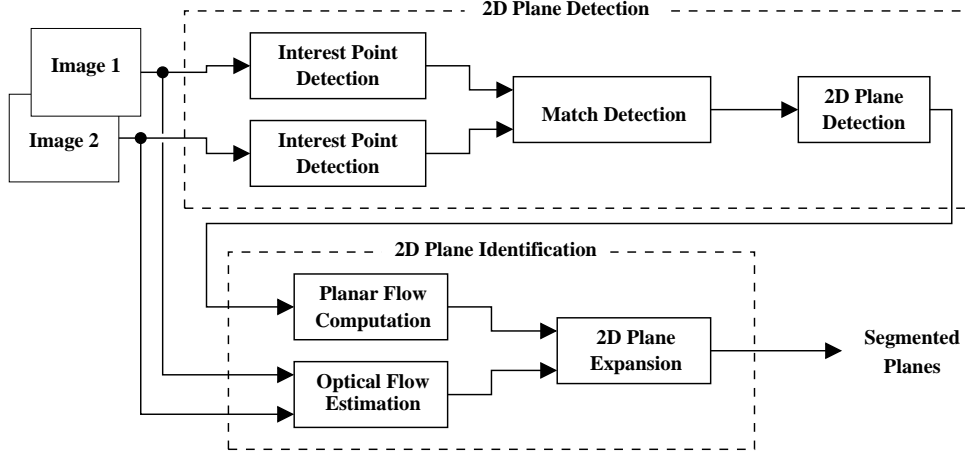


Figure 1: Block diagram of the proposed system.

matched pairs of points in the set M . At the end of clustering stage, only planes with a number of points above a certain threshold are considered. All other ones are discarded.

B. 2D Plane Expansion and Identification

In most cases, planes present in an image acquired by a robot vision system can be classified into two categories: *ground floor* and *obstacles*. The detection procedure provides multiple planar regions in the 2D image space. However, the detected planes are small and not identified regions.

In order to overcome this problem, we propose an optical flow based system for the expansion of all previously detected planes in a scene. Moreover, the proposed identification system in this work suppose that the ground floor is the predominant plane in the image, and obstacles are represented by small secondary planes.

Each affine homography computed on the detection stage determines the movement of the pixels that belong to the same plane. This movement can be represented by the planar flow $\mathbf{v}_p = (v_{x_p}, v_{y_p})$ and can be computed by

$$\mathbf{v}_p = \mathbf{q}' - \mathbf{q} = \mathbf{H}_A \mathbf{q} - \mathbf{q}. \quad (13)$$

The same movement can also be represented by the estimated optical flow $\mathbf{v}_e = (v_{x_e}, v_{y_e})$ from two consecutive images. Thus, the detected planes can be expanded by comparing the movements described by the planar flow and the estimated flow.

The detected planes are enlarged by including pixels whose the error between \mathbf{v}_e and \mathbf{v}_p is below a certain threshold. The error between the two flow vectors can be defined by the equation

$$err_v = \sqrt{(v_{x_e} - v_{x_p})^2 + (v_{y_e} - v_{y_p})^2}. \quad (14)$$

At the end, the number of pixels labeled as belong to each plane is used by the identification process. The biggest

plane is identified as the ground plane. All other ones are identified as obstacles.

The entire procedure of expansion and identification of the detected planes is described by the Algorithm 1.

Algorithm 1 Algorithm for expansion and identification of the segmented planes.

Given:

H_m : set of homographies that represent each detected plane;

T_v : error threshold between the estimated flow \mathbf{v}_e and the planar flow \mathbf{v}_p ;

Define:

$err_v(\mathbf{v}_e, \mathbf{v}_p)$: error between the planar flow and the estimated flow;

Estimate the optical flow \mathbf{v}_e for all pixels of the image;

for $i =$ each pixel of the first image **do**

for $j =$ each homography of H_m **do**

 Compute the planar flow $\mathbf{v}_p(i) = H_m(j)\mathbf{q}(i) - \mathbf{q}(i)$;

if $err_v(\mathbf{v}_e(i), \mathbf{v}_p(i)) < T_v$ **then**

 Associate the pixel i as belonging to the plane defined by the homography j ;

end if

end for

end for

The biggest plane is the ground plane, and all the others are obstacles;

V. EXPERIMENTAL RESULTS

In this section, we report some experimental results from real image data. Several colored image sequences of indoor and outdoor scenes were acquired by a unique moving camera. Scenes with planes at different positions and orientations were chosen. The system was tested on both indoor and

outdoor image sequences. Due to paper length restrictions, only a small part of these results are shown.

Different parameters of the system were empirically adjusted at each stage of the entire process of the 3D plane reconstruction. The following sections discuss each one of them. At the clustering procedure, only one parameter is adjustable. The reprojection error threshold was empirically chosen as $T_e = 5.0$. The value of T_e is dynamically updated during the clustering process. Each matched pair of points in M is assigned to the best homography in H_p , based on the reprojection error. At the end, only clusters with a number of points above a certain threshold are considered as detected planes.

The following step consists of the expansion and identification procedure. The optical flow \mathbf{v}_e was estimated using the method proposed in Section III. Also, the planar flow \mathbf{v}_p is computed for all pixels in the image using each homography resulting from the clustering scheme. According to the Equation 14, an error threshold was empirically chosen and, for each pixel, it is verified if it belongs to some detected plane.

Finally, the plane with the biggest number of points corresponds to the ground plane. All other ones are labeled as obstacles.

In order to evaluate the accuracy of the plane segmentation system, we use an error measure. The major planes were manually detected and compared with the planes detected by the proposed system, and the error measured by

$$err_p = 100 \frac{\sum_{x,y} |D_m(x,y) - D_s(x,y)|}{\sum_{x,y} 1} \quad (15)$$

where $D_m(x,y)$ and $D_s(x,y)$ are equal to 1 or 0 if the point (x,y) belongs or not to the manually detected plane (D_m) or to the plane detected by the system (D_s).

Figures 2 and 3 illustrates the major segmented planes in the indoor and outdoor images. Table I presents the computed error in the segmentation process.

Table I: Error (%), false-positives measures FP (%) and false-negatives measures FN (%) computed on the plane identification procedure to the left and right indoor images of Figure 2, and for outdoor image of Figure 3.

Image	Obstacle			Ground		
	Error	FP	FN	Error	FP	FN
Indoor (left)	5.18	1.33	3.85	11.55	2.13	9.42
Indoor (right)	2.19	0.77	1.42	13.40	4.75	8.65
Outdoor	17.14	5.91	11.23	11.92	3.19	8.73

In order to allow the path planning of the mobile robot, the system was also tested using a long image sequence. Figure 4 and Table II show the results.

VI. CONCLUSIONS AND FUTURE WORKS

In this paper we present a system for plane segmentation. The system is divided in two parts. First, a detection

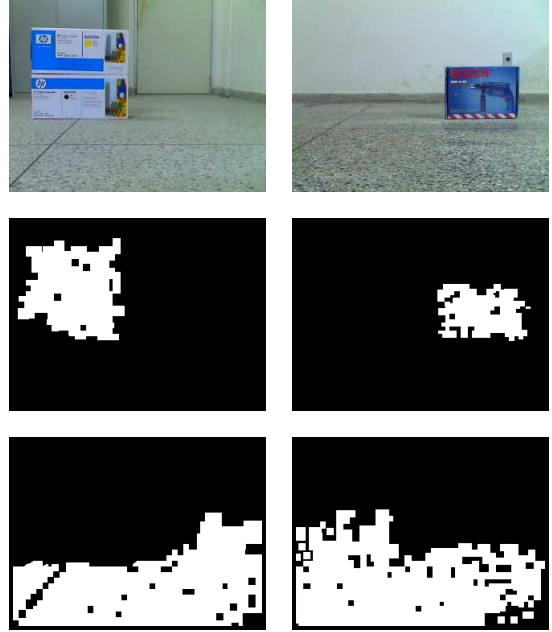


Figure 2: Results of the plane identification procedure for indoor images.

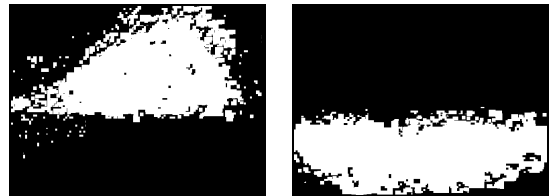


Figure 3: Results of the plane identification procedure for outdoor image.

procedure that consists of a clustering scheme based on the computation of homographies using the model affine. Second, an expansion and identification procedure based on comparing the estimated optical flow and the planar flow. The optical flow is estimated from color information, and the planar flow is obtained from the homographies that represent each detected plane.

In the proposed system, any error in one module is fixed or discarded by the following ones. Furthermore, we emphasize that the segmentation was performed from two images acquired by a monocular vision system, where the distance traveled by the camera between two acquisitions is unknown.

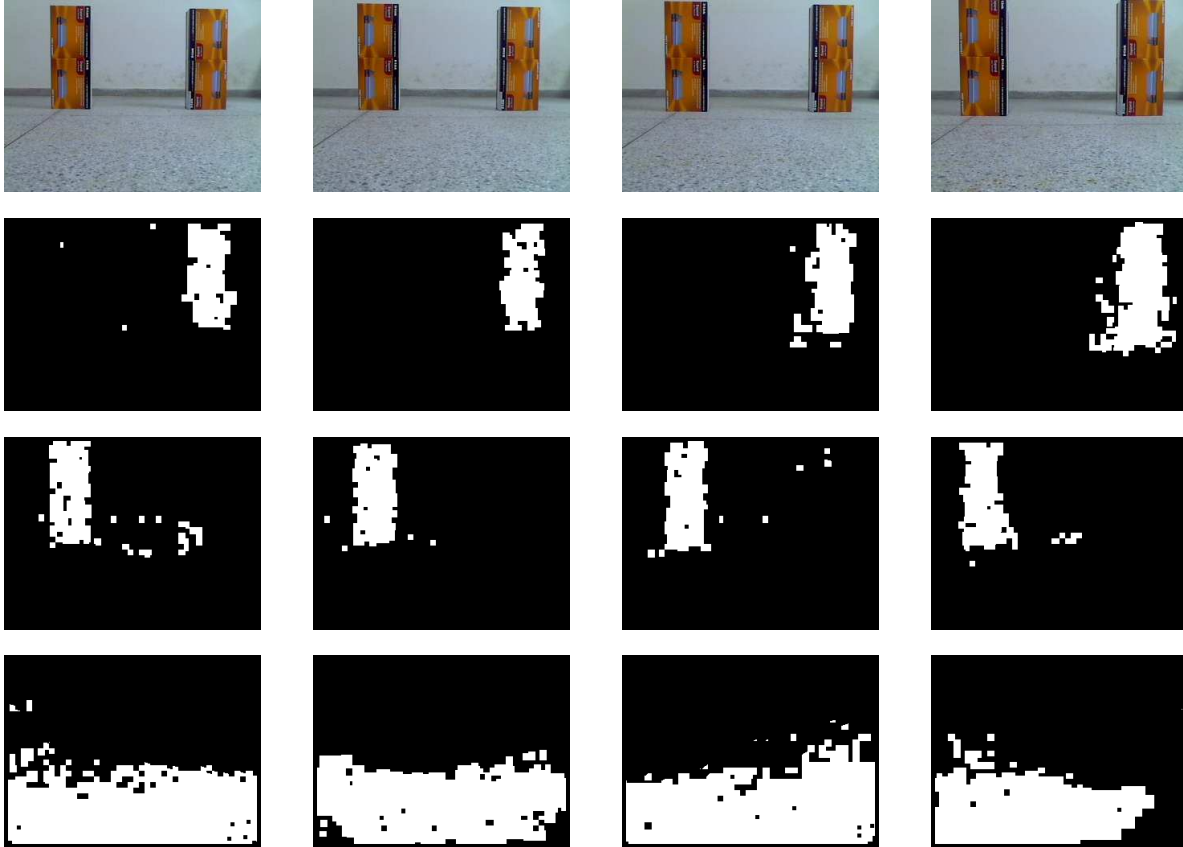


Figure 4: Identified planes in the 1, 11, 21 and 31 frames of an image sequence. The first row is the original image. The middle rows are the obstacles, and the bottom row is the ground plane.

Table II: Error (%), false-positive measures FP (%) and false-negatives measures FN (%) computed on the plane identification procedure to the image sequence of Figure 4.

Frame	Right Obst.		Left Obst.		Ground	
	Error	FP	Error	FN	Error	FP
01	2.26	1.17	3.05	1.14	9.19	0.67
11	2.21	0.58	2.54	1.69	11.46	0.48
21	2.88	1.52	2.27	1.56	10.54	2.18
31	5.06	3.88	4.19	3.30	18.02	1.33

The identification procedure is based on the number of pixels belonging to each segmented plane. Some restrictions about the environment are done. The ground floor is assumed to be a planar surface, and this is the dominant plane in the scene. At the end, each plane is labeled as ground plane or obstacle.

Finally, the system was tested using indoor and outdoor image sequences and presented good results. The results demonstrate the reliability of the proposed system, whereas the obtained error in the expansion process is acceptable. In order to solve the problem of capturing images of close obstacles, we could consider the ground plane as the plane nearest the bottom edge of the image.

Future work will be concentrated at the 3D reconstruction of the segmented planes for path planning and navigation of the mobile robot. Here, if the odometer data about the robot's movement is available, it is possible to recover the scale factor related to the determination of the 3D position of the planes. In addition, the performance of the system will be evaluated.

REFERENCES

- [1] D. Sinclair and A. Blake, "Quantitative planar region detection," *Int. J. Comput. Vision*, vol. 18, no. 1, pp. 77–91, 1996.
- [2] K. Okada, S. Kagami, M. Inaba, and H. Inoue, "Plane segment finder: Algorithm, implementation and applications," in *IEEE International Conference on Robotics and Automation*, vol. 2. IEEE Computer Society, 2001, pp. 2120–2125.
- [3] Q. He and C.-H. H. Chu, "Planar surface detection in image pairs using homographic constraints," in *ISVC (1)*, ser. Lecture Notes in Computer Science, vol. 4291. Springer, 2006, pp. 19–27.
- [4] J. Piazzini and D. Prattichizzo, "Plane detection with stereo images," in *IEEE International Conference on Robotics and Automation*. IEEE Computer Society, 2006, pp. 922–927.

- [5] G. Silveira, E. Malis, and P. Rives, "Real-time robust detection of planar regions in a pair of images," in *International Conference on Intelligent Robots and Systems*. IEEE Computer Society, 2006, pp. 49–54.
- [6] R. Rodrigo, Z. Chen, and J. Samarabandu, "Feature motion for monocular robot navigation," in *Information and Automation, 2006. ICIA 2006. International Conference on*, 2006, pp. 201–205.
- [7] N. Ohnishi and A. Imiya, "Dominant plane detection from optical flow for robot navigation," *Pattern Recognition Letters*, vol. 27, no. 9, pp. 1009–1021, 2006.
- [8] A. Agarwal, C. V. Jawahar, and P. J. Narayanan, "A survey of planar homography estimation techniques," Centre for Visual Information Technology, Tech. Rep. IIT/TR/2005/12, 2005.
- [9] B. Horn and B. Schunck, "Determining optical flow," *Artificial Intelligence*, vol. 16, no. 1-3, pp. 185–203, August 1981.
- [10] B. Lucas and T. Kanade, "An iterative image registration technique with an application to stereo vision," in *IJCAI81*, 1981, pp. 674–679.
- [11] N. Ohta, "Optical flow detection by color images," *IEEE International Conference On Image Processing*, pp. 801–805, Sep. 1989.
- [12] N. Ohta and S. Nishizawa, "How much does color information help optical flow computation?" *IEICE Transactions on Information and Systems - Oxford Journal*, vol. 5, pp. 1759–1762, 2006.
- [13] J. Barron and R. Klette, "Quantitative color optical flow," in *Proceedings of 16th International Conference on Pattern Recognition*, vol. 4, 2002, pp. 251–255.
- [14] K. R. T. Aires, A. M. Santana, and A. A. D. d. Medeiros, "Optical flow using color information: preliminary results," in *Proceedings of the 2008 ACM Symposium on Applied Computing*. Fortaleza, CE, Brazil: ACM, Mar. 2008, pp. 1607–1611.
- [15] K. R. T. Aires, H. d. J. Araújo, and A. A. D. d. Medeiros, "Plane detection from monocular image sequences," in *Proceedings of 8th IASTED International Conference on Visualization and Image Processing - VIIP2008*. Mallorca, Spain: ACTA Press, Sep. 2008.
- [16] K. Mikolajczyk and C. Schmid, "A performance evaluation of local descriptors," *IEEE Transactions on Pattern Analysis and Machine Intelligence*, vol. 27, no. 10, pp. 1615–1630, 2005.
- [17] C. Harris and M. Stephens, "A combined corner and edge detection," in *Proceedings of The Fourth Alvey Vision Conference*, 1988, pp. 147–152.
- [18] D. Lowe, "Distinctive image features from scale-invariant keypoints," in *International Journal of Computer Vision*, vol. 20, 2003, pp. 91–110.
- [19] F. P. Preparata and M. I. Shamos, *Computational Geometry: An Introduction (Monographs in Computer Science)*. Springer, August 1985.